

**UCLA**

**UCLA Electronic Theses and Dissertations**

**Title**

Estrogen Receptor Alpha Regulates Ucp1-Independent Thermogenesis Through Serca2b-Mediated Calcium Cycling in Brown Adipose Tissue

**Permalink**

<https://escholarship.org/uc/item/7r71f3jp>

**Author**

Ma, Alice Mengyuan

**Publication Date**

2024

Peer reviewed|Thesis/dissertation

UNIVERSITY OF CALIFORNIA

Los Angeles

Estrogen Receptor Alpha Regulates Ucp1-Independent Thermogenesis Through  
Serca2b-Mediated Calcium Cycling in Brown Adipose Tissue

A thesis submitted in partial satisfaction of the requirements for the degree Master of  
Science in Physiological Science

by

Alice Mengyuan Ma

2024

© Copyright by  
Alice Mengyuan Ma  
2024

## ABSTRACT OF THE THESIS

Estrogen Receptor Alpha Regulates Ucp1-Independent Thermogenesis Through  
Serca2b-Mediated Calcium Cycling in Brown Adipose Tissue

by

Alice Mengyuan Ma

Master of Science in Physiological Science

University of California, Los Angeles, 2024

Professor Andrea L. Hevener, Co-Chair

Professor Claudio Javier Villanueva, Co-Chair

Obesity is a complex and prevalent condition in the United States and is associated with higher rates of mortality driven by cardiovascular disease, type 2 diabetes, and certain types of cancer. Prior research showed that expression of adipose tissue *Esr1*, which encodes estrogen receptor alpha ( $ER\alpha$ ), inversely associates with adiposity in both humans and rodents. Studies of an adipose-specific *Esr1* knockout mouse model showed that  $ER\alpha$  regulates energy homeostasis in white adipose tissue (WAT) and brown adipose tissue (BAT) via coordinated control of mitochondrial DNA replication and fission-fusion-mitophagy dynamics. However, the molecular mechanisms of the

metabolic-protective role of ER $\alpha$  in adipose tissue, specifically in BAT, are not clear. Herein, we investigated the metabolic role of ER $\alpha$  by overexpressing ESR1 through both female and male adipose-specific ER $\alpha$  transgenic mice. We found that overexpression of ESR1 in adipose tissue of female mice ameliorated high-fat diet-feeding-induced weight gain and elevated core body temperatures. Further examination of male mice with adipose overexpression of ER $\alpha$  showed that the protective role of ER $\alpha$  is hormone dependent. Elevated core body temperatures did not coordinate with Ucp1 expression, a key regulator of thermogenesis, indicating that ER $\alpha$  regulates thermogenesis in BAT via Ucp1-independent action. Moreover, studies showed that estradiol (E2) elevated calcium cycling, and E2-ER $\alpha$  transcriptionally regulates expression of calcium transporter Serca2b in primary brown adipocytes as a means of thermogenesis. Together, we found a novel role of ER $\alpha$  in regulating a noncanonical thermogenesis pathway enhancing calcium cycling via the calcium transporter Serca2b in BAT.

The thesis of Alice Mengyuan Ma is approved.

Zhenqi Zhou

Stephanie Correa

Claudio Javier Villanueva, Committee Co-Chair

Andrea L. Hevener, Committee Co-Chair

University of California, Los Angeles

2024

## Table of Contents

Abstract	ii
Committee Page	iv
List of Figures and Tables	vi
Acknowledgements	vii
Introduction	1
Materials and Methods	3
Results	9
Figures	14
Discussion	24
References	26

## List of Figures and Tables

Antibody List	7
Primer List	8
Figure 1	14
Figure 2	16
Figure 3	18
Figure 4	19
Figure 5	21
Figure 6	22



## Acknowledgements

To my parents and my family, thank you for always supporting me and my dreams. To Peter, thank you for being my best friend and my rock. To Dr. Hevener and ZQ, thank you for teaching me how to love science. To all the friends I've made along the way, thank you for brightening every day.

## **Introduction**

Obesity remains a prevalent health concern in the United States and contributes significantly to increased morbidity and mortality due to cardiovascular disease, diabetes, cancer, and more<sup>1</sup>. The primary physiological cause of obesity is an overconsumption of nutrients and calories coupled with an underutilization of energy stores resulting in an accumulation of excess adipose tissue that underlies metabolic dysfunction<sup>2</sup>. Examinations in sex differences in disease prevalence show that pre-menopausal women are protected from metabolic-related diseases like cardiometabolic dysfunction when compared to men, while post-menopausal women make up a growing subpopulation of overweight adults, more so than their age-matched male counterparts<sup>2,3</sup>. Studies of menopausal women show that in the years leading up to the final menstrual period, the average rate of fat mass increase nearly doubles<sup>3</sup>. Mechanisms implicated in obesity in post-menopausal women include ovarian failure during the menopausal transition, where women undergo a dramatic decrease in estrogen levels during menopause, leading to detrimental effects on metabolism and changes in body fat distribution, reduced glucose tolerance, increased blood pressure, and other comorbidities that often culminate in obesity<sup>4</sup>.

Obesity is characterized by an excess of adiposity, but not all forms of adipose tissue are metabolically detrimental. Brown adipose tissue (BAT) makes up a unique subpopulation of adipocytes that are mitochondrially enriched and play a central role in non-shivering thermogenesis. This thermogenesis is a critical method of metabolic heat production canonically characterized by the uncoupling of mitochondrial respiration from ATP synthesis. Activation of thermogenesis in BAT has been shown to contribute to

improvements in metabolic homeostasis and function and play a critical role in maintaining thermal homeostasis<sup>5</sup>. Many studies have shown that core body temperature is higher in female rodents and humans compared to their male counterparts, and post-menopausal women have a lower core temperature than pre-menopausal women, suggesting a dynamic sex hormone-driven regulation of body temperature<sup>6-11</sup>. Additionally, women in the first 14 days of the menstrual cycle are more likely to have lower core body temperatures than women in the last 14 days, a pattern that coincides with the peak in cyclic estradiol levels, further suggesting a strong positive association between estradiol levels, body temperature, and brown adipose tissue activation<sup>7,12</sup>.

Our previous studies have shown that expression of adipose tissue *Esr1*, which encodes estrogen receptor alpha (*ERα*), inversely associates with adiposity in both humans and rodents<sup>13</sup>. We also found that *Esr1* is a requisite for uncoupled respiration thermogenesis by *Ucp1*, a key regulator of BAT thermogenesis<sup>13</sup>. However, the molecular mechanisms of the metabolic-protective role of *ERα* in adipose tissue, especially in brown adipose tissue, remain inadequately understood. Herein, we investigated the metabolic role of *ERα* in brown adipose tissue by overexpression *Esr1* in both female and male mice and identified a novel role of *ERα* in regulating a noncanonical thermogenesis pathway through enhancing calcium cycling via the calcium import protein *Serca2b*.

## **Materials and Methods**

### **Animal Care**

All animal care and experimentation procedures were approved by the University of California, Los Angeles Institutional Animal Care and Use Committee (IACUC). Mice were maintained on a 12-hour light/dark cycle from 6am to 6pm at ambient temperature (approximately 22°C) with controlled humidity (approximately 45%) in pathogen-free conditions. Food and water consumption and animal welfare were monitored daily by the Division of Laboratory Animal Medicine at UCLA. Prior to organ harvest, mice were euthanized by isoflurane overdose followed by cervical dislocation. This is an approved method according to the recommendations of the panel on Euthanasia of the American Veterinary Medical Association.

### **Mouse Lines**

A mouse line exhibiting an adipose tissue-specific overexpression of ER $\alpha$  (aER<sup>T9</sup>) was generated using Rosa-ER $\alpha$  flox mice which contain an ER $\alpha$  construct inserted in the Rosa26 locus preceded by a STOP codon flanked by LoxP sites. This mouse was crossed with a transgenic mouse expressing a tamoxifen inducible Cre recombinase under the control of the Adipoq gene promoter (The Jackson Laboratory Strain #025124). Successfully genotyped pups were injected with a single-dose of 2mg of tamoxifen (Sigma, T5648) at 8 weeks of age and placed on a 45% kcal high-fat diet (Research Diets, D12451) for 8 weeks post-injection. A second, brown adipose tissue-specific mouse line (bER<sup>T9</sup>) was generated using the Rosa-ER $\alpha$  flox mice injected with AAV-Ucp1-Cre to induce overexpression exclusively in the BAT. bER<sup>T9</sup> mice were also

maintained on a high-fat diet following AAV administration. Male bER<sup>Tg</sup> mice were treated with exogenous estradiol in the form of a  $\beta$ -17 estradiol pellet (Innovative Research of America, E-121) surgically inserted subcutaneously while mice were under anesthesia. All control mice were Rose-ER $\alpha$  flox animals that did not contain the Cre recombinase. All mice studied were of C57BL/6J background between 4 and 6 months of age.

### **Phenotypic Measurements**

Body temperature measurements were conducted using an implantable RFID microchip (BMDS IMI-1000 Transponder) inserted subcutaneously while animals were under anesthesia. Body temperature measurements were taken using a wireless reader (BMDS DAS-8006 IUS). Body composition was examined by NMR scanning (Bruker). Oxygen consumption, carbon dioxide production, food and water consumption, and ambulatory movement were determined using metabolic chambers with singly housed animals (Oxymax Metabolic Chambers, Columbus Instruments). Glucose tolerance test was conducted following a 6-hour fast and an intraperitoneal injection of 1g/kg dextrose using HemoCue Glucose Chips (Glucose 201). Insulin tolerance test was conducted following a 16-hour fast and an intraperitoneal injection of 0.75U/kg of insulin.

### **Cell Culture**

Immortalized brown adipocytes were cultured in high-glucose Dulbecco's Modified Eagle Medium (Corning, 10-013-CM) supplemented with 10% fetal bovine serum (Corning, 35-011-CV) and penicillin/streptomycin until full confluency. At

confluence, growth medium was switched for DM1 consisting of high-glucose Dulbecco's Modified Eagle Medium supplemented with 10% FBS, 1uM dexamethasone (Sigma, D4902), 0.5mM IBMX (Sigma, I7018), 125uM indomethacin (Sigma, I7378), 5ug/mL insulin (Sigma, I5500), 1uM rosiglitazone (Cayman, 71740), and 2nM T3 (Sigma, T2877) for two days of differentiation. During final three days of differentiation, DM1 was switched to DM2 consisting of high-glucose, phenol red-free Dulbecco's Modified Eagle Medium (Cytiva, SH30284.01) supplemented with 10% charcoal-stripped FBS (Gibco, 12676029), 5ug/mL insulin (Sigma, I5500), 1uM rosiglitazone (Cayman, 71740), and 2nM T3 (Sigma, T2877). Cells were treated with 10nM E2 (Sigma, E8875) or 10nM PPT (Tocris, 1426) as needed. Cells were used for protein immunoblot analysis, qPCR analysis, or in vitro calcium assay.

### **In Vitro Calcium Assay**

Cells were cultured and differentiated in optical clear bottom, black 96-well plates (Thermo, 165305). On day 3 of differentiation, cells were treated with GCaMP<sup>er</sup> 14 for 24 hours to label endoplasmic reticulum calcium ions. Prior to imaging, cells are treated with E2 or PPT and activation of thermogenesis pathways was induced by 1uM norepinephrine (Sigma, A7257). Imaging was done using the Biotek Lionheart FX microscope.

### **Immunoblot Analysis**

Mouse tissue samples or cell pellets were homogenized or sonicated in radioimmunoprecipitation assay (RIPA) lysis buffer containing freshly added protease

(cOmplete EDTA-free, Roche). All lysates were clarified, centrifuged, and resolved by SDS–polyacrylamide gel electrophoresis. After transfer, PVDF membranes were probed with the listed antibodies, and then imaged separately using a Bio-Rad ChemiDoc XRS imaging system. The exposure time was adjusted and the densitometric analysis was performed using the BioRad Quantity One or ImageLab software.

### **Quantitative Reverse Transcription PCR**

Tissues or cells were homogenized using TRIzol reagent (Invitrogen, 15596018) and RNA was isolated and further cleaned using RNeasy columns (Qiagen, 74106). Complementary DNA synthesis was performed using 1mg of RNA with iScript™ cDNA Synthesis (Biorad, 1708890). qPCRs were conducted using PowerUP SYBR Green Master Mix (Thermo, 2919059). All qPCRs were performed using QuantStudio 5 (Invitrogen). Quantification of a given gene, expressed as relative mRNA level compared with control, was calculated after normalization to a standard housekeeping gene (18S). Primer pairs were designed using Primer Express 2.0 (Applied Biosystems) or previously published sequences. Primer sets were checked for specificity using BLAST (Basic Local Alignment Search Tool; National Center for Biotechnology Information).

### **Chromatin Immunoprecipitation**

Immortalized brown adipocytes were cultured and differentiated as described above. Approximately  $8 \times 10^6$  cells were used for treatment with vehicle or 10nM E2 for 24 hours with three technical replicates per condition. Cells were crosslinked using 1%

formaldehyde, lysed, and pelleted for sonication. Sonication was conducted using the Covaris truCHIP Chromatin Shearing Kit. Immunoprecipitation was conducted using the Recombinant Anti-Estrogen Receptor Alpha Antibody [E115] - CHIP Grade (Abcam ab32063). Phenol-chloroform extraction was conducted to precipitate the DNA, and samples were used for qPCR in a 1:25 dilution for input and 1:3 dilution for IP samples.

## Statistics

Values presented are expressed as means  $\pm$  SEM unless otherwise indicated. Statistical analyses were performed using Student's t test when comparing two groups of samples or Two-way analysis of variance (ANOVA) for identification of significance within and between groups using GraphPad Prism 10 (GraphPad Software). Significance was set a priori at  $P < 0.05$ .

## Antibody Catalog

<b>Protein</b>	<b>Source</b>	<b>Catalog</b>
Atp6	Cell Signaling	70262S
Ckb	abcam	ab151579
CoxIV	Cell Signaling	4850S
Drp1	Cell Signaling Technology	8570S
ERalpha	Sigma	06-935
Gapdh	Cell Signaling Technology	5174S
Hmgb1	abcam	ab18256
Hsp90	Cell Signaling Technology	4874
Ip3r	Cell Signaling Technology	8568S
Mfn1	ProteinTech	13798-1-AP
Mfn2	abcam	ab56889
Nd1	abcam	ab181848
Oxphos	Mitosciences	MS604
Ryr2	abcam	ab302716
Serca2b	abcam	ab3625
Ucp1	Cell Signaling Technology	14670S
Vdac1	Cell Signaling Technology	4866S



## Primer Catalog

Gene	Forward	Reverse
18S	CGCCGCTAGAGGTGAAATTCT	CGAACCTCCGACTTTTCGTTCT
Acox1	GCCCAACTGTGACTTCCAT	GGCATGTAACCCGTAGCACT
Atp2a2a	CTGTGGAGACCCTTGTTGT	CAGAGCACAGATGGTGGCTA
Atp2a2b	CTGTGGAGACCCTTGTTGT	CAGAGCACAGATGGTGGCTA
Cidea	TCTGCAATCCCATGAATGTC	GTGGCTGATAGGGCAGTGAT
Ckb	AAGTTCTCGGAGGTGCTCAA	AGTTTCACTCCGTCCACCAC
Ckm	CATGGAGAAGGGAGGCAATA	GACGAAGGCGAGTGAGAATC
Ckmt1	TCTGGGTGAATGAGGAGGAC	TTGGGAAGCGGTTATCTTTG
Ckmt2	GCTGGTGTCCACGTTAGGAT	ATCTGCCGATCCGATCTATG
Dio2	ATTCAGGATTGGAGACGTGC	ATGCTGACCTCAGAAGGGC
Elovl3	CCAACAACGATGAGCAACAG	CGGGTTAAAAATGGACCTGA
Ip3r1	GAAGCAGCATGTGTTCTGA	GGTCTACCTCTGCAGCCAAG
Ip3r2	CGGAGCTACTGTTCCAGAG	ATTCGCCGTAATGTGCTACC
mtAtp6	CCACACACAAAAGGACGAA	GAAGGAAGTGGGCAAGTGAG
mtCo3	GCAGGATTCTTCTGAGCGTTCT	GTCAGCAGCCTCCTAGATCATGT
mtNd4	GCCTGATTACTGCCACTAATA	GGTTCCTCATCGGGTAATAA
mtNd6	GATATACGACTGCTATAGCTA	ACAACATATATTGCCGCTAC
Ndufs1	CACTCGTTCCACCTCAGCTA	GACGGCTCCTCTACTGCCT
Ndufs4	GTGTCCCGAGTCTGGTTGTC	CAATGTCAGTGTCGGCTGAG
Pgc1a	TGAGGACCGCTAGCAAGTTT	TGAAGTGGTGTAGCGACCAA
Polg	TAGCTGGCTGGTCCAAGAGT	CGACGTGGAGGTCTGCTT
Ryr2	GCGAGCTGGCTACTATGACC	CGTTGCTAATGCTCACGAAA
Sdha	TACTACAGCCCCAAGTCT	TGGACCCATCTTCTATGC
Serca1	TGAATTCGATGGCCTGGACT	ACATGGACAGGCAGATGGAA
Serca3	ATATCCTGGCCAAGATCCGG	CATGACCACTCGAATGCCAG
Tnap	TGGGTGGCGGCCGAAATACAT	GGAGGGGTCAAGGGCCAGCAGTT
Ucp1	GGAAAGGGACGACCCCTAATC	GGAAAGGGACGACCCCTAATC

## **Results**

### **Adipose-specific overexpression of ER $\alpha$ in female mice confers protection against diet-induced weight gain.**

To investigate the role of ER $\alpha$  in adipose tissue metabolism, we generated adipose-specific ER $\alpha$  overexpression mice that showed approximately 1.3-fold increase in ER $\alpha$  protein expression in brown adipose tissue with corresponding increases in gene expression across brown and white adipose tissue depots (Fig 1a). Overexpression of ER $\alpha$  was induced with tamoxifen injection at 8 weeks of age where tamoxifen-activated Cre excised the STOP codon preceding ER $\alpha$ . This was paired with administration of a high-fat diet ad libitum. aER<sup>Tg</sup> mice began to show decreased weight gain beginning at three weeks (Fig 1b). Four weeks following ESR1 induction in BAT, fat mass was significantly reduced. No difference in lean mass was detected between the genotypes. (Fig 1c). Whole-body metabolism measured by glucose and insulin tolerance tests showed improved glucose homeostasis and insulin sensitivity in aER<sup>Tg</sup> mice compared to control mice (Fig 1d-e). Consistent with improved metabolic function, white adipose (gonadal WAT and inguinal WAT) and brown adipose tissue show decreases in adipocyte size and area (Fig 1f-g).

### **Female aER<sup>Tg</sup> mice exhibit improved whole body metabolic function and increased energy expenditure and thermogenesis.**

Next, we determined the effect of adipose-specific ER $\alpha$  overexpression on whole-body energy metabolism. Mice were individually housed in metabolic chambers for indirect calorimetric measurements of O<sub>2</sub> consumption and CO<sub>2</sub>. Day and night

VO<sub>2</sub>, VCO<sub>2</sub>, and energy expenditure (EE) were elevated in aER<sup>Tg</sup> mice compared to control mice with no change in respiratory exchange rate (RER), food consumption, and activity (Fig 2a-f). Core body temperature showed consistent elevations in aER<sup>Tg</sup> mice compared to control mice (Fig 2g). In a second mouse model, we selectively overexpressed ER $\alpha$  in the BAT of mice (bER<sup>Tg</sup>). bER<sup>Tg</sup> female mice phenocopied aER<sup>Tg</sup> female mice in differential weight gain and core body temperatures (Fig 2h-i). Cold exposure induces Ucp1-mediated non-shivering thermogenesis in BAT in order to maintain core body temperature<sup>15</sup>. Female bER<sup>Tg</sup> mice also showed significantly higher body temperatures following cold exposure at 4 degrees Celsius, suggesting a higher degree of thermogenic capacity (Fig 2j). Taken together, these data suggest differential regulation of thermogenesis as a result of adipose-specific ER $\alpha$  overexpression and point to ER $\alpha$ 's role in regulating thermogenesis in adipose metabolism.

### **Male bER<sup>Tg</sup> mice shows requisite ligand presence in protection against diet-induced obesity.**

In male bER<sup>Tg</sup> mice, we saw that ER $\alpha$  overexpression in brown adipose tissue does not confer metabolic protection from diet-induced weight gain or drive differential body temperature (Fig 3a-b). However, treatment of these male mice with an exogenous supply of estradiol delivered by a surgically implanted subcutaneous estradiol pellet showed phenocopying of female models and their ability to adopt metabolic protection. Following estradiol treatment, male overexpression mice began to show differential weight gain and trending body temperature changes, as well as

significant increases in VO<sub>2</sub> and VCO<sub>2</sub> (Fig 3a-d). These data confirm that ER $\alpha$ 's role in BAT thermogenesis is estradiol dependent and displays sexually dimorphic regulation.

### **ER $\alpha$ regulates Ucp1-independent thermogenesis in brown adipose tissue.**

Uncoupling protein 1 (Ucp1) is a canonical regulator of thermogenesis that is expressed in the mitochondria of brown adipocytes. It uncouples cellular respiration and mitochondrial ATP synthesis to generate energy in the form of released heat<sup>16</sup>. As such, we examined Ucp1 gene and protein expression in the BAT of overexpression and control mice. Interestingly, we did not see a significant upregulation of Ucp1 gene or protein expression between overexpression and control mice (Fig 4a-b). Other key mitochondrial proteins including those involved in oxidative phosphorylation and fission/fusion dynamics also showed no change (Fig 4c-e). Several mitochondrially encoded genes did show upregulation, as well as select browning genes (Fig 4b). These data suggest that ER $\alpha$ 's regulation of thermogenesis operates in a Ucp1-independent fashion that circumvents mitochondrially derived uncoupling.

### **ER $\alpha$ overexpression results in upregulation of calcium cycling genes and proteins.**

Several Ucp1-independent pathways of thermogenesis have been identified where mechanisms of creatine cycling, calcium cycling, and lipid oxidation can increase heat production while producing ATP sinks<sup>17</sup>. In assessing the BAT of aER<sup>Tg</sup> and control animals, we observed no differences in protein or gene expression of key creatine cycling genes (Fig 5a). However, we did observe increases in key calcium import and

export genes (Fig 5b-c). There are several key calcium import and export proteins, including sarcoplasmic/endoplasmic reticulum Ca<sup>2+</sup>-ATPase 2b (Serca2b, encoded by genes *Atp2a2a* and *Atp2a2b*), inositol 1,4,5-trisphosphate receptors (*Ip3r1* and *Ip3r2*), and ryanodine receptor 2 (*Ryr2*). These proteins work in concert to regulate the movement of calcium throughout the endoplasmic reticulum, where futile calcium cycling in and between the sarco-endoplasmic reticulum acts as a mechanism of thermogenesis<sup>18</sup>. Elevations of these calcium proteins were seen in vivo, in both our female *aER<sup>Tg</sup>* and *bER<sup>Tg</sup>* models and in our male *bER<sup>Tg</sup>* mice following estradiol pelleting, suggesting a calcium cycling-dependent mechanism of thermogenesis that may be regulated by ER $\alpha$  in BAT (Fig 5b-d). Additionally, overexpressing ER $\alpha$  in brown adipocytes in culture with an adenovirus showed consistent increases in Serca2b protein expression levels (Fig 5e).

### **ER $\alpha$ transcriptionally regulates Serca2b gene expression in brown adipose tissue.**

ER $\alpha$  regulates estrogen-sensitive genes by binding DNA on specific estrogen response elements (EREs) preceding coding sequences of target genes. By screening publicly available predicted EREs, we identified two potential EREs in Serca2b's promoter region, further suggesting direct regulation of Serca2b by ER $\alpha$ . To experimentally confirm this relationship, we conducted chromatin immunoprecipitation (ChIP) pull-down of ER $\alpha$ . Using immortalized brown adipocytes treated with estradiol, we confirmed the ability of estradiol-activated ER $\alpha$  to bind to one of the two predicted EREs of *Atp2a2* (Fig 6a). This finding confirms the direct, transcriptional regulation of

Serca2b by ER $\alpha$ . Consequently, treatment of immortalized brown adipocytes with PPT, an ER $\alpha$ -specific agonist, significantly elevated Serca2b protein expression and Atp2a2a and Atp2a2b gene expression (Fig 6b). These findings suggest that ER $\alpha$ 's ability to regulate whole-body energy expenditure through thermogenesis is a result of its transcriptional regulation of Serca2b and the subsequent modulation of futile calcium cycling.

Our in vitro models also suggest ER $\alpha$  has specificity to upregulate Serca2b gene expression while downregulating Serca1 gene expression (Fig 6c). Inversely, administration of diarylpropionitrile (DPN), an ER $\beta$ -specific agonist, to brown adipocytes showed no change on Serca2b gene expression but induction of Serca1 gene expression (Fig 6d). These findings suggest that estrogen receptors regulate Serca proteins uniquely across isoforms in brown adipose tissue and may represent a potential future endeavor in assessing the role of estrogen receptors on calcium cycling.

### **Activation of ER $\alpha$ induces increases calcium flux in vitro.**

We used an ER-localizing GCaMP calcium biosensor to label calcium ions in immortalized brown adipocytes. Administering PPT to brown adipocytes showed significant upregulation of calcium flux following norepinephrine stimulation (Fig 6e). Blocking ER $\alpha$  with a specific Esr1-interfering RNA ablated PPT-driven calcium flux, suggesting that ER $\alpha$  is a prerequisite for inducing calcium flux by norepinephrine stimulation (Fig 6f).

## Figures

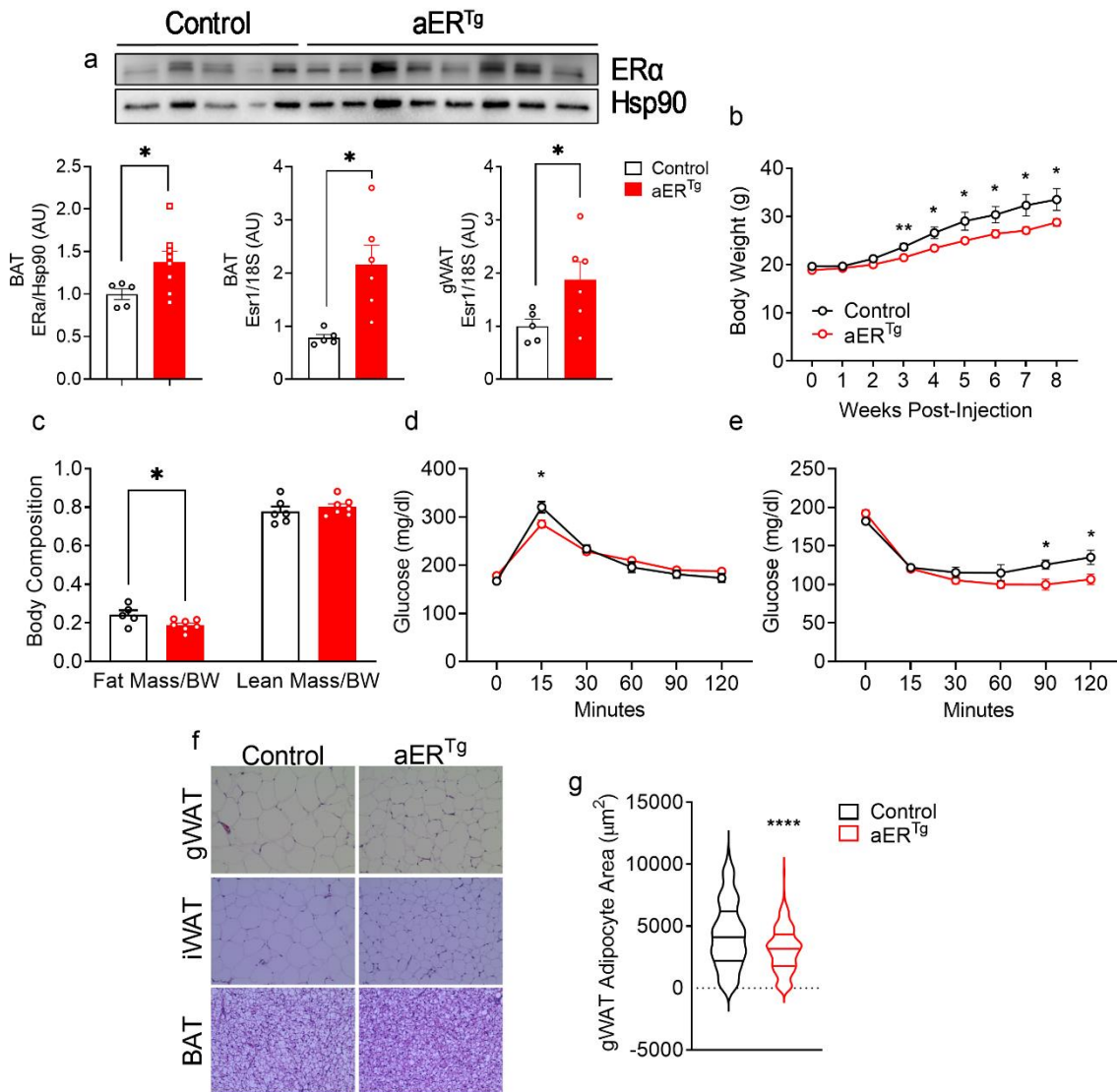


**Figure 1: Overexpression of adipose tissue ERα in female mice protects against diet-induced obesity.**

a) Adipose-specific overexpression of ERα confirmed with protein immunoblot and gene expression in brown and white adipose tissue depots. b) Body weight measurements of aER<sup>Tg</sup> and control mice over 8 weeks post induction of ERα overexpression and high fat diet feeding. c) Body composition measurements presented as ratio of lean or fat mass

to total body weight collected at 4 weeks post-injection. d) Glucose tolerance test administered at 4 weeks post-injection. e) Insulin tolerance test administered at 7 weeks post-injection. f) Histological sections of gWAT, iWAT, and BAT from control and aER<sup>Tg</sup> mice.



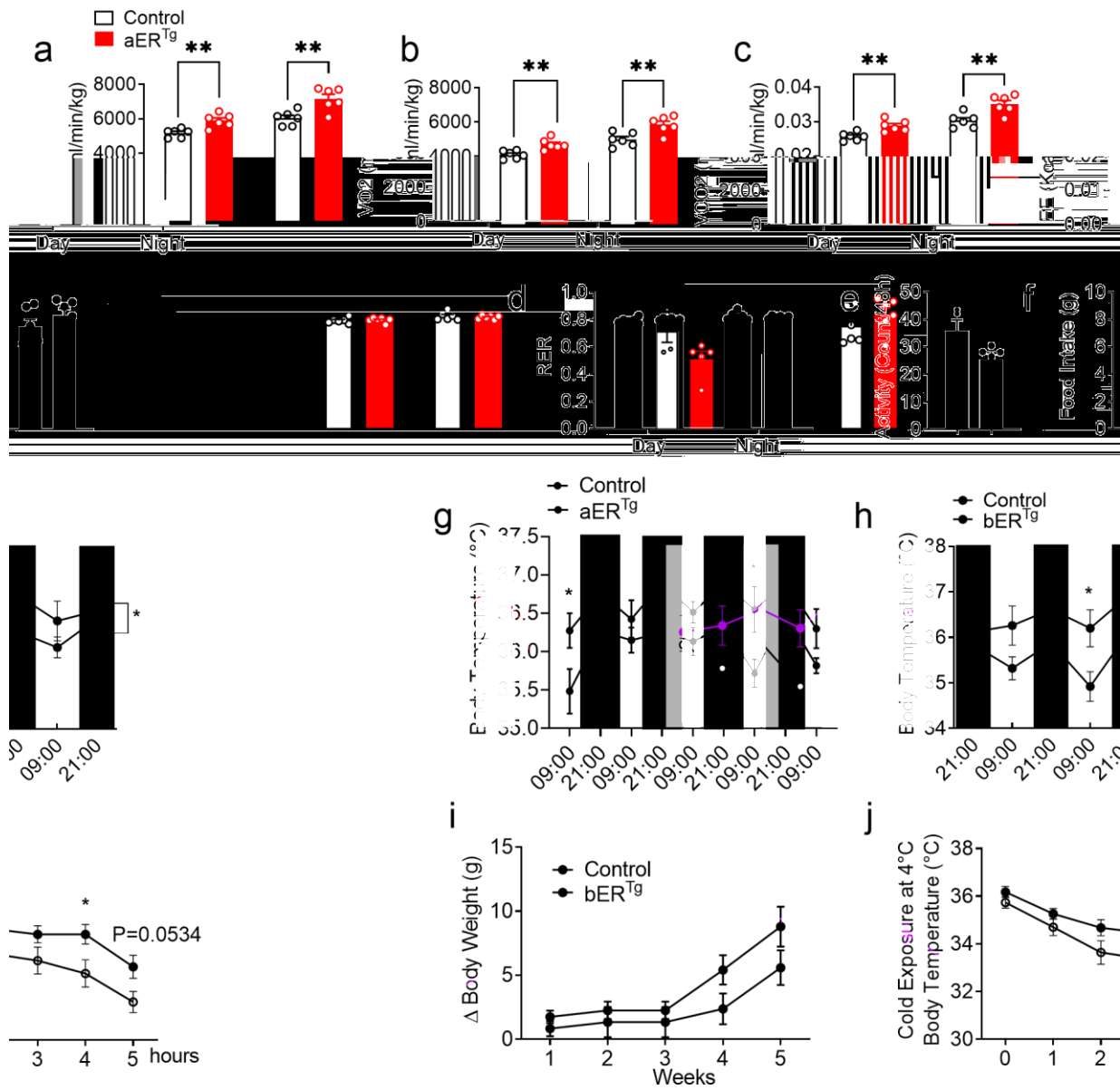


**Figure 2: Female aER<sup>Tg</sup> and bER<sup>Tg</sup> mice have improved whole-body metabolism, increased energy expenditure, and core body temperature.**

a-f) Metabolic chamber data from aER<sup>Tg</sup> female mice and control female mice showing  $\dot{V}O_2$ ,  $\dot{V}CO_2$ , EE, RER, activity, and food intake. g-h) Core body temperature measurements taken across day and night phases in female aER<sup>Tg</sup> mice and female bER<sup>Tg</sup> mice, respectively. i) Change in body weight in female bER<sup>Tg</sup> mice and control

mice. j) Core body temperature during cold exposure at 4°C in female bER<sup>Tg</sup> mice and control mice.

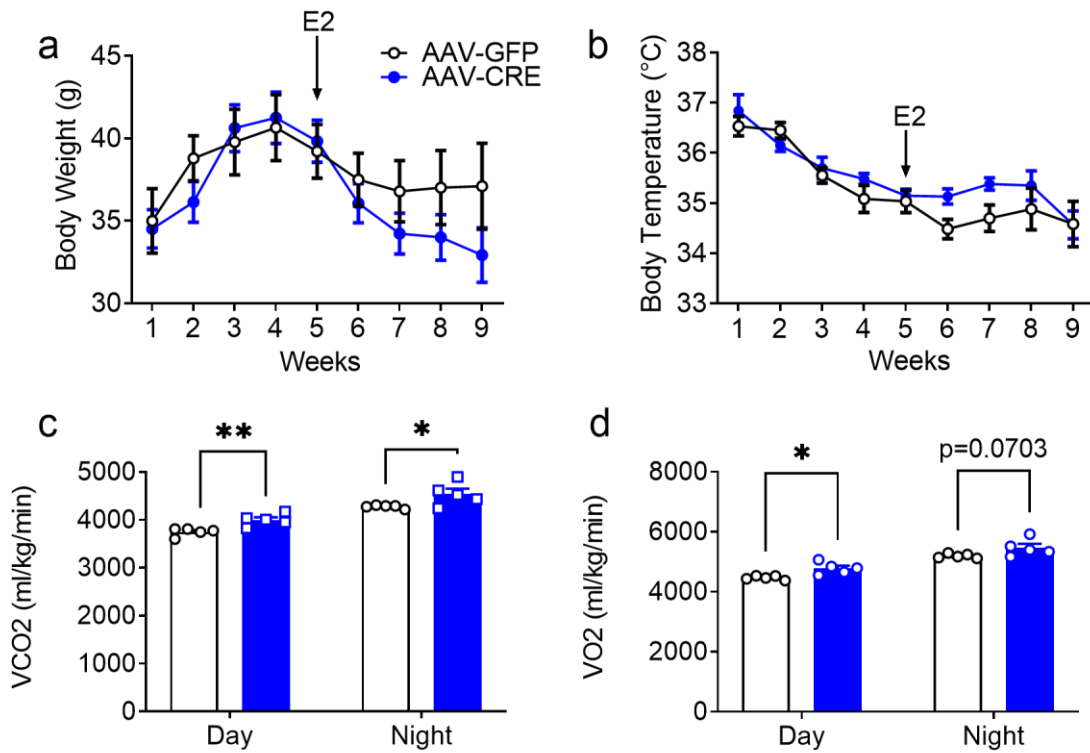


**Figure 3: Male bERT<sup>g</sup> mice show that ER $\alpha$  protection against diet-induced obesity requires activation by estradiol.**

a-b) Body weight and core body temperature in male bERT<sup>g</sup> mice before and after pelleting with estradiol. c-d) Metabolic chamber data from male bERT<sup>g</sup> mice after pelleting with estradiol.

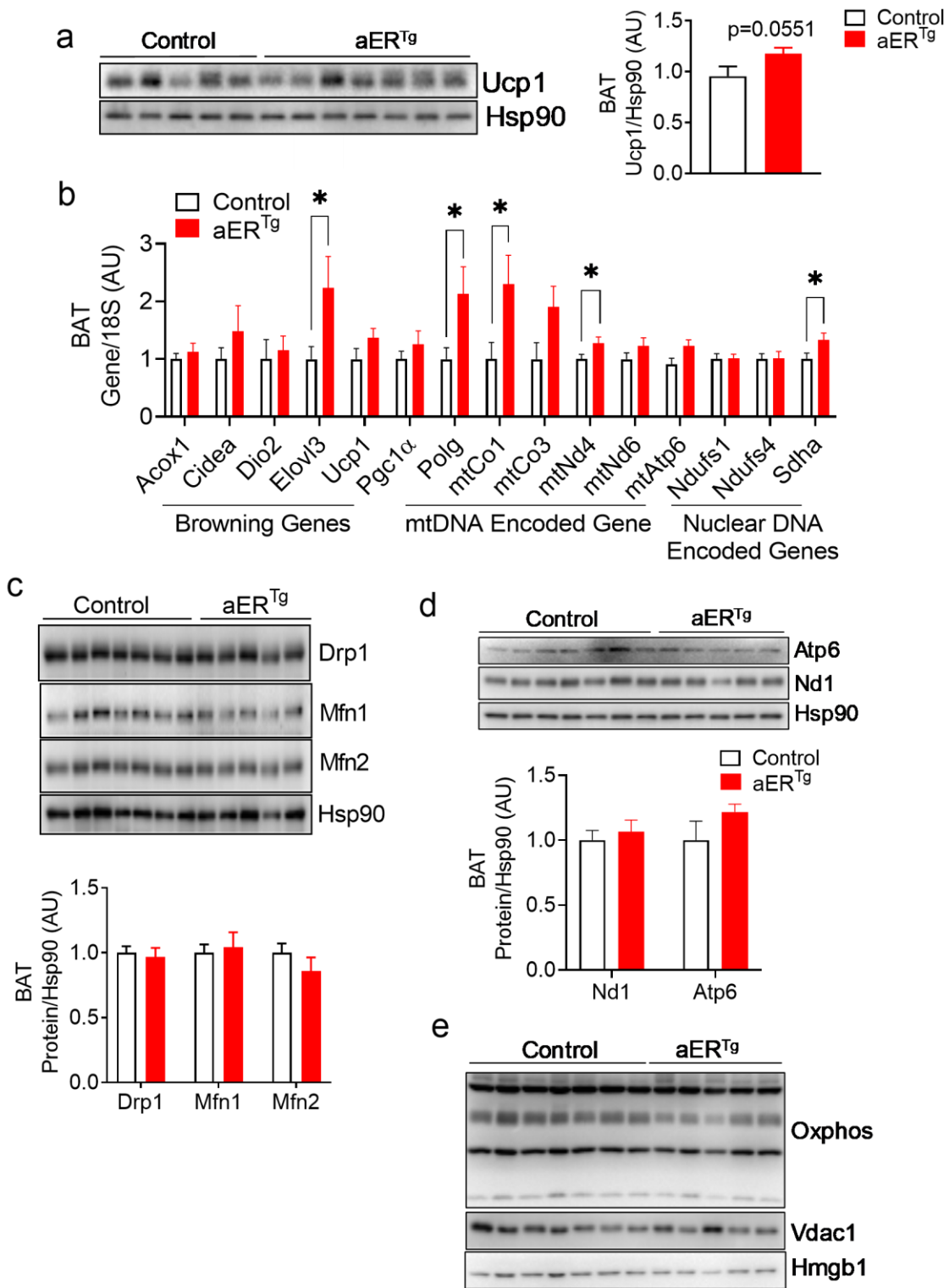


**Figure 4: ER $\alpha$  overexpression-induced thermogenesis is Ucp1-independent.**

a) Ucp1 protein expression in BAT of female aER<sup>Tg</sup> mice. b) Gene expression analysis in BAT of female aER<sup>Tg</sup> mice for browning genes, including Ucp1, mitochondrial and nuclear encoded genes. c-e) Protein expression in BAT of female aER<sup>Tg</sup> mice for select mitochondrial proteins.

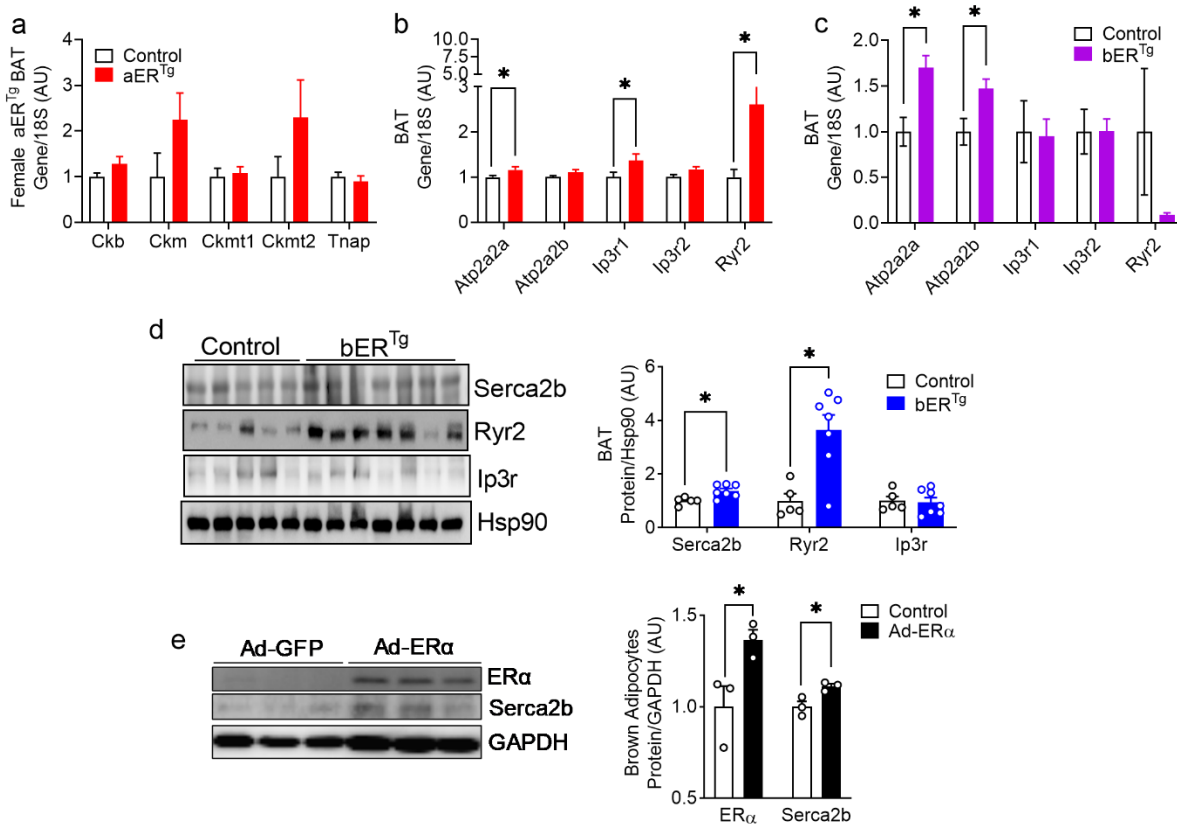


**Figure 5: ER $\alpha$  overexpression induces upregulation of calcium cycling genes and proteins in BAT.**

a) Expression of creatine cycling genes in BAT of female aER<sup>Tg</sup> mice. b) Expression of calcium cycling genes BAT of female aER<sup>Tg</sup> mice. c) Expression of calcium cycling genes BAT of female bER<sup>Tg</sup> mice. d) Expression of calcium cycling proteins in BAT of male bER<sup>Tg</sup> mice. e) Expression of ER $\alpha$  and Serca2b in cultured brown adipocytes with overexpression of ER $\alpha$  by adenovirus.

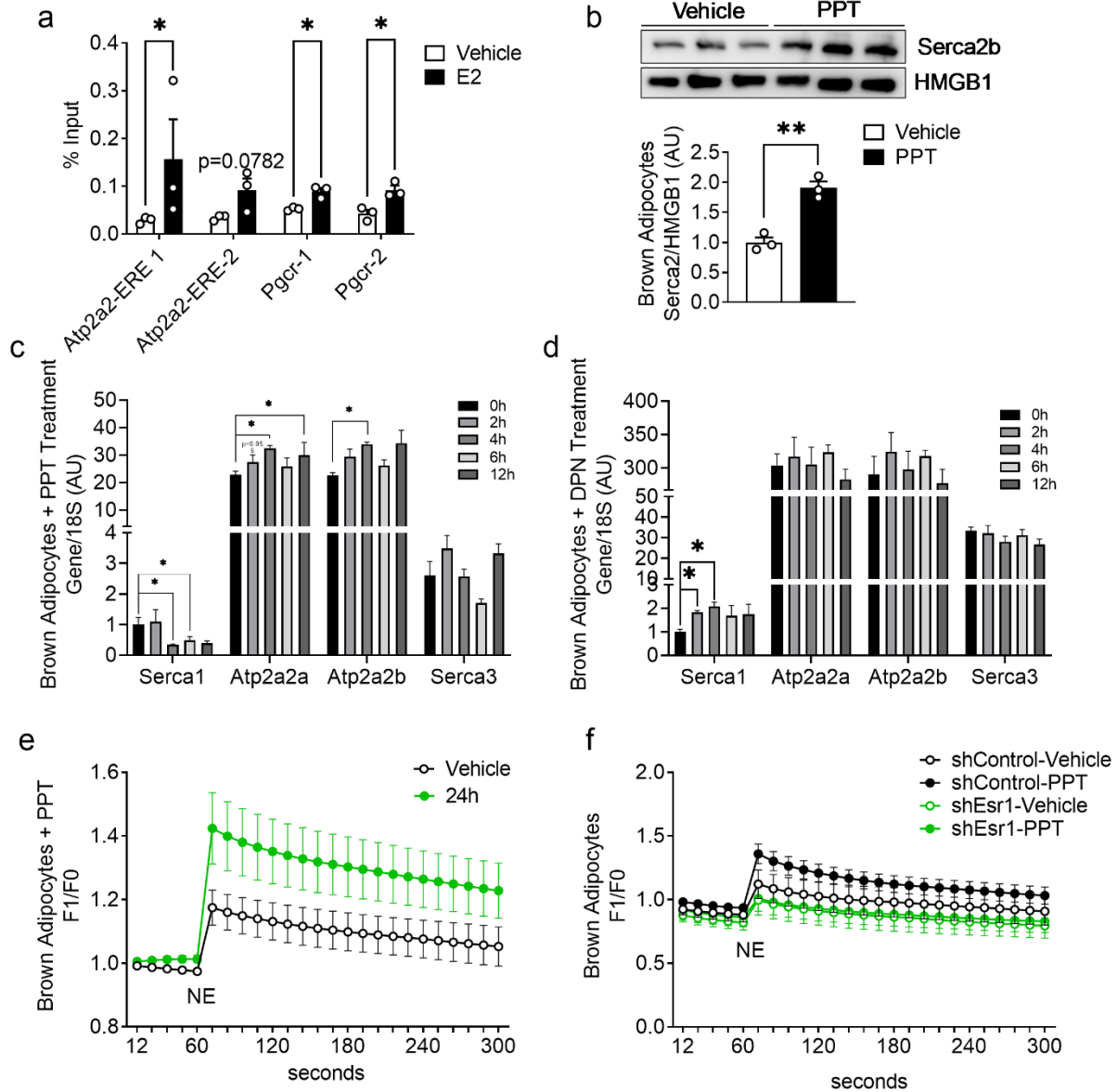


**Figure 6: ER $\alpha$  transcriptionally regulates Serca2b to induce calcium flux-mediated thermogenesis in brown adipocytes.**

a) ChIP-qPCR of Atp2a2 EREs and Pgc1-2 (positive controls) in brown adipocytes treated with E2. b) Protein expression of Serca2b in PPT-treated brown adipocytes. c) Serca1-3 gene expression in PPT-treated brown adipocytes. d) Serca1-3 gene expression in DPN-treated brown adipocytes. e) Labeled calcium flux in PPT-treated

brown adipocytes stimulated with norepinephrine. f) Labeled calcium flux in PPT-treated brown adipocytes with knockdown of ER $\alpha$  by shEsr1.



## **Discussion**

Excess caloric consumption and underutilization of energy results in an accumulation of fat that underlies the development of obesity and metabolic dysfunction. Sex differences in weight gain and metabolic disease show that women's protection against obesity wanes with menopause and evidence of circulating estradiol's role in inducing brown adipose tissue thermogenesis further implicate its primary receptor, estrogen receptor alpha, in adipose tissue metabolism. Our findings from mouse brown adipose tissue corroborated these studies where female mice exhibiting an overexpression of ER $\alpha$  in adipose tissue conferred protection against diet-induced obesity. Consistent with the sexual dimorphism of ER $\alpha$ 's regulatory role, we saw that male mice exhibiting brown adipose tissue-specific overexpression of ER $\alpha$  did not offer protection against diet-induced weight gain until exogenous estradiol was supplied. Taken together, these data confirm that ER $\alpha$ 's role in protecting against excess adiposity is ligand-dependent and sexually dimorphic.

Assessments in whole body metabolism in our models suggested that ER $\alpha$ 's ability to protect against diet-induced obesity derives from its ability to upregulate energy expenditure through BAT thermogenesis. Previous findings implicated ER $\alpha$ 's prerequisite role to Ucp1 thermogenesis<sup>13</sup>, but our findings here suggested that overexpression of ER $\alpha$  does not induce Ucp1 activity further above baseline, suggesting a mechanism of Ucp1-independent thermogenesis. In recent findings, several mechanisms of Ucp1-independent thermogenesis have been identified where ATP sinks from creatine, lipid, or calcium cycling have all been implicated as mechanisms of thermogenesis regulated by pathways beyond Ucp1<sup>17</sup>. Specifically, calcium cycling by

the Serca2-Ryr2 pathway was identified as a mechanism of ATP-dependent thermogenesis in beige adipocytes<sup>18</sup>. Our findings recapitulated these results in BAT and found a novel regulatory function of ligand-dependent ER $\alpha$  in calcium-driven thermogenesis.

Serca proteins have three differentially expressed isoforms that have been implicated in regulation of calcium cycling across many tissues. Serca1 is widely expressed in fast-twitch skeletal muscle, Serca2a is found in cardiac/slow-twitch muscles, Serca2b is expressed in smooth muscle and non-muscle tissues, and Serca3 is also found in non-muscle tissues<sup>19</sup>. Through our in vitro brown adipocyte model, we established ER $\alpha$  specificity to upregulation of Serca2b gene expression while downregulating Serca1. Furthermore, we showed ER $\beta$  specificity to upregulation of Serca1. This suggests unique transcriptional regulation of the Serca isoforms by estrogen-sensitive receptors and presents an interesting direction for regulation of calcium flux across tissues.

In conclusion, our study found that ER $\alpha$  regulates brown adipose tissue thermogenesis through calcium-mediated flux. ER $\alpha$  transcriptional regulation of Serca2b allows for activation of Ucp1-independent thermogenesis. This role of ER $\alpha$  displays sexual dimorphism through its requisite ligand binding. Our results provide further insights into sex differences underlying obesity prevalence and implicates the role of ER $\alpha$  in metabolic function. As such, ER $\alpha$  action in brown adipose tissue may be a potential therapeutic target to combat obesity and metabolic dysfunction.

## **References**

1. Aronne, L. J. Classification of obesity and assessment of obesity-related health risks. *Obes Res* **10**, (2002).
2. Kautzky-Willer, A., Harreiter, J. & Pacini, G. Sex and Gender Differences in Risk, Pathophysiology and Complications of Type 2 Diabetes Mellitus. *Endocr Rev* **37**, 278 (2016).
3. Greendale, G. A. *et al.* Changes in body composition and weight during the menopause transition. *JCI Insight* **4**, (2019).
4. Kozakowski, J., Gietka-Czernel, M., Leszczynska, D. & Majos, A. Obesity in menopause – our negligence or an unfortunate inevitability? *Prz Menopauzalny* **16**, 61 (2017).
5. Bartelt, A. & Heeren, J. Adipose tissue browning and metabolic health. *Nat Rev Endocrinol* **10**, 24–36 (2014).
6. Yanovich, R., Ketko, I. & Charkoudian, N. Sex differences in human thermoregulation: Relevance for 2020 and beyond. *Physiology* **35**, 177–184 (2020).
7. Kim, H., Richardson, C., Roberts, J., Gren, L. & Lyon, J. L. Cold hands, warm heart. *The Lancet* **351**, 1492 (1998).
8. Kaciuba-Uscilko, H. & Grucza, R. Gender differences in thermoregulation. *Curr Opin Clin Nutr Metab Care* **4**, (2001).
9. Sanchez-Alavez, M., Alboni, S. & Conti, B. Sex- and age-specific differences in core body temperature of C57Bl/6 mice. *Age (Omaha)* **33**, 89 (2011).

10. Neff, L. M. *et al.* Core body temperature is lower in postmenopausal women than premenopausal women: potential implications for energy metabolism and midlife weight gain. **5**, 151–154 (2016).
11. Molnar, G. W. Body temperatures during menopausal hot flashes. <https://doi.org/10.1152/jappl.1975.38.3.499> **38**, 499–503 (1975).
12. Reed, B. G. & Carr, B. R. The Normal Menstrual Cycle and the Control of Ovulation. *Endotext* (2018).
13. Zhou, Z. *et al.* Estrogen receptor  $\alpha$  controls metabolism in white and brown adipocytes by regulating Polg1 and mitochondrial remodeling. *Sci Transl Med* **12**, 8096 (2020).
14. Henderson, M. J. *et al.* A Low Affinity GCaMP3 Variant (GCaMPer) for Imaging the Endoplasmic Reticulum Calcium Store. *PLoS One* **10(10)**: e0139273., (2015).
15. Okamatsu-Ogura, Y. *et al.* UCP1-dependent and UCP1-independent metabolic changes induced by acute cold exposure in brown adipose tissue of mice. (2020) doi:10.1016/j.metabol.2020.154396.
16. Nedergaard, J. *et al.* UCP1: the only protein able to mediate adaptive non-shivering thermogenesis and metabolic inefficiency. *Biochim Biophys Acta* **1504**, 82–106 (2001).
17. Roesler, A. & Kazak, L. UCP1-independent thermogenesis. *Biochemical Journal* **477**, 709–725 (2020).
18. Ikeda, K. *et al.* UCP1-independent signaling involving SERCA2b-mediated calcium cycling regulates beige fat thermogenesis and systemic glucose homeostasis. (2017) doi:10.1038/nm.4429.

19. MacLennan, D. H., Rice, W. J. & Green, N. M. The mechanism of Ca<sup>2+</sup> transport by sarco(endo)plasmic reticulum Ca<sup>2+</sup>-ATPases. *Journal of Biological Chemistry* **272**, 28815–28818 (1997).